Structure of Fundamental Solutions of a Conservation Law without Convexity

by

Yong Jung Kim, Youngran Lee

Applied Mathematics
Research Report
08 - 02
March 12, 2008

DEPARTMENT OF MATHEMATICAL SCIENCES

KAIST 한국과학기술원
Korea Advanced Institute of Science and Technology

ARMA manuscript No.
(will be inserted by the editor)

Structure of fundamental solutions of a conservation law without convexity ⋆

Yong-Jung Kim, Young-Ran Lee

Abstract

This note is devoted to reveal the structure of signed fundamental solutions of a conservation law without the convexity assumption. It is assumed that the flux is in $C^1(\boldsymbol{R})$ and has a finite number of inflection points. Fundamental solutions of the case have been constructed in [5] employing convex and concave envelopes. This construction provides useful information on the structure of the fundamental solution in terms of the envelopes and we clarify the dynamics of a fundamental solution using this structural information. We classify the types of shocks, rarefaction waves and their interactions to reach the final stage of its asymptotics. A complete example of such a dynamics is given with a full characteristic map.

1. Introduction

This note is written under a single purpose to clarify the dynamics of a fundamental solution to a conservation law without convexity. If the flux is convex, the structure of a solution to a conservation law is well understood. In particular one may employ the Lax-Hopf transformation to obtain the solution almost explicitly. If the flux is not convex, we do not have such a luxury and the solution may show a completely different behavior. Due to the complexity of this non-convex case, understanding its dynamics is limited in compare with a convex case.

In this paper we let $u(x,t)$ be a solution to a conservation law

$$u_t + f(u)_x = 0, \quad x \in \boldsymbol{R},\ t > 0, \tag{1}$$

⋆ This work was supported by the Korea Science and Engineering Foundation(KOSEF) grant funded by the Korea government(MOST) (No.R01-2007-000-11307-0).

where the flux f is in $C^1(\boldsymbol{R})$ and satisfies the following hypotheses:

$$\begin{gathered} \textit{the flux } f(u) \textit{ has a finite number of inflection points} \\ \textit{and} \\ f(u)/|u| \to \infty \quad \text{as} \quad |u| \to \infty. \end{gathered} \tag{H1}$$

If a bounded solution is considered, then the flux value as $|u| \to \infty$ does not make any difference and hence one may always assume the second hypothesis without loss of generality. The first hypothesis is due to iterative arguments in the construction of a fundamental solution. Assuming this, one may obtain a fundamental solution in a finite number of steps [5].

Under a similar hypothesis of a finite number of inflection points, the existence and uniqueness of bounded solutions to (1) were given by Ballou [1] and the zero viscosity limit by Tang et al [9] in the class of piecewise smooth weak solutions. The regularity and asymptotic behavior of the solution have been obtained by Dafermos [2] and Liu [7]. The structure of a solution has been studied in [1,2] for the case with a single inflection point. However, understanding the structure of a solution is far less satisfactory in compare with the convex case. One of the reasons is that we do not have a handy tool to view the structure of the solution. For example the rigorous use of the method of generalized characteristics is "lengthy and even torturous". Another reason is the lack of complete examples that provide the essential feature of its dynamics. In this paper we survey the structure of a fundamental solution in detail in terms of the dynamics of convex and concave envelopes.

Since we are interested in a fundamental or a source-type solution to the conservation law (1), we consider the corresponding initial condition given by the Dirac-measure,

$$u(x,0) = M\delta(x), \quad M \in \boldsymbol{R}. \tag{2}$$

We consider a weak solution that satisfies the Oleinik entropy condition:

$$l(u) \le f(u) \text{ for all } u_l < u < u_r \text{ and } l(u) \ge f(u) \text{ for all } u_r < u < u_l, \tag{3}$$

where u_r and u_l are the right and the left hand side limits at a possible discontinuity point (x,t) and $l(u)$ is the line segment connecting $(u_r, f(u_r))$ and $(u_l, f(u_l))$, i.e.,

$$l(u) = \frac{f(u_r) - f(u_l)}{u_r - u_l}(u - u_l) + f(u_l), \;\; u_l = \lim_{y \uparrow x} u(y,t), \;\; u_r = \lim_{y \downarrow x} u(y,t).$$

Recently Kim and Ha [5] constructed a signed fundamental solution of a conservation law in a more or less explicit way under (H1). From this construction one may find basic structures of a fundamental solution, which are summarized in Lemma 1. Using this structural lemma we clarify what the types of shocks and rarefaction waves of a fundamental solution are, how they appear, interact and vanish, and how the solution reaches the final stage of the long time asymptotics.

A bounded solution is unique for an initial value problem with a bounded initial value. However, a fundamental solution is not unique in general. Liu and Pierre [8] considered source-solutions under a hypothesis

$$f(u) \geq 0 \quad \text{for} \quad u \in \boldsymbol{R}, \tag{H2}$$

and showed that the signed fundamental solution to (1,2) is unique. We extend this uniqueness to a case without (H2), Theorem 1. Let $N_{0,q}(x,t)$ be the unique positively signed fundamental solution corresponding to $M = q > 0$ and $N_{p,0}(x,t)$ be the negative one with $M = -p < 0$. The fundamental solution of a conservation law is known as an N-wave for the Burgers equation case, which has been easily extended to a case with convex flux. Therefore, $N_{0,q}(x,t)$ and $N_{p,0}(x,t)$ are generalized signed N-waves under a flux without convexity.

In this paper we mostly consider the structure of the signed fundamental solution under the hypotheses (H1). We will classify the types of shocks and rarefaction waves in Sections 3 and 5 and their possible dynamics such as branching and merging of shocks in Section 4. Then eventually a complete scenario of the evolution of a fundamental solution is given in Section 6 in terms of the evolution of convex-concave envelopes (see Figures 6 and 7). The dynamics of the fundamental solution studied in this paper can be observed by numerical computations. One may find the dynamics of the fundamental solution studied the paper from Figures 8 and 9.

In Section 7 the structure of a fundamental solution is considered under the extra hypothesis (H2). We can easily see that the positive and negative parts evolve independently and hence

$$N_{p,q}(x,t) = N_{p,0}(x,t) + N_{0,q}(x,t), \quad q = M + p, \tag{4}$$

are also solutions to the problem (1,2) under (H2). Hence a fundamental solution is not unique if solutions with a sign-change are allowed.

2. Preliminaries and scaling invariance of source-type solutions

One can easily check that, after an appropriate change of variables which counts the velocity of the flow at $u = 0$, we may assume

$$f(0) = f'(0) = 0 \tag{5}$$

without loss of generality. The uniqueness of a signed fundamental solution is shown for a positive flux (H2), see [8]. In the followings we easily extend this uniqueness under (H1) only.

Theorem 1 (uniqueness of a signed fundamental solution). *Suppose that the flux $f \in C^1(\boldsymbol{R})$ satisfies (H1). Then there exists at most one signed fundamental solution to (1,2) which has the same sign as the one of M.*

Proof. It is enough to show the uniqueness of a positive solution assuming $M > 0$. The assumption (H1) and (5) imply that there exists $b > 0$ such that $f(u) \geq -bu$ for all $u \geq 0$. Let $\varphi(u) = f(u) + bu$. Then $\varphi(0) = 0$ and $\varphi(u) \geq 0$ for all $u \geq 0$. Therefore, a positive solution to

$$u_t + \varphi(u)_x = 0, \qquad u(x,0) = M\delta(x) \tag{6}$$

is unique (see Theorem 1.1 [8]). Let u be a positive solution to (1,2) and v be its translation given by $v(x,t) = u(x - bt, t) \geq 0$. Then,

$$v_t + \varphi(v)_x = u_t - bu_x + f(u)_x + bu_x = 0.$$

One can easily check that v satisfies the entropy condition (3) if u does. Therefore, v is a solution to (6). Let $\tilde{u}$ be another positive solution to (1,2) and $\tilde{v}$ be given similarly by $\tilde{v}(x,t) = \tilde{u}(x - bt, t)$. Then, since a positive solution to (6) is unique, $v(x,t) = \tilde{v}(x,t)$ and hence $u(x,t) = \tilde{u}(x,t)$.

Now we show a scaling argument using this uniqueness theorem. Let $u(x,t) = N_{0,q}(qx, qt)$ with $q > 0$. Recall that $N_{0,q}(x,t)$ is the positive solution of (1,2) with $M = q$. Then $u_t = q\partial_t N_{0,q}(qx,qt)$, $u_x = q\partial_x N_{0,q}(qx,qt)$, and hence

$$u_t + f'(u)u_x = q\partial_t N_{0,q}(qx,qt) + qf'(N_{0,q}(qx,qt))\partial_x N_{0,q}(qx,qt) = 0.$$

Furthermore, since

$$\int \phi(x)u(x,0)dx = \int \phi(x)N_{0,q}(qx,0)dx = \int \phi(y/q)\delta(y)dy = \phi(0),$$

$u(x,t)$ is the positive source type solution with $M = 1$. Therefore, the uniqueness of a signed solution implies that

$$N_{0,1}(x,t) = N_{0,q}(qx,qt), \quad x \in \boldsymbol{R},\ t > 0. \tag{7}$$

Similarly, for negative N-waves, we have

$$N_{1,0}(x,t) = N_{p,0}(px,pt), \quad x \in \boldsymbol{R},\ t > 0, \tag{8}$$

for any $p > 0$. These relations indicate that it is enough to study the structures of $N_{0,1}(x,t)$ and $N_{1,0}(x,t)$ only. We will consider the positive case only and hence the solution $u(x,t)$ here is basically the positive N-wave $N_{0,1}(x,t)$. However, for the notational convenience, we stick to use $u(x,t)$ for the solution of (1,2) with $M > 0$. The negative case can be considered similarly and is omitted.

It is well known that a weak solution should satisfy the Rankine-Hugoniot jump condition at any discontinuity curve $x = s(t)$ which is given by

$$s'(t) = \frac{f(u_r) - f(u_l)}{u_r - u_l}, \quad u_l = \lim_{y \uparrow s(t)} u(y,t),\ u_r = \lim_{y \downarrow s(t)} u(y,t). \tag{9}$$

On the other hand one may consider a characteristic line $x = \xi(t)$ that emanates from a point (x_0, t_0) that satisfies

$$\xi'(t) = f'(u(\xi(t), t)), \quad \xi(t_0) = x_0, \tag{10}$$

where the domain of the characteristic depends on the continuity and on the types of discontinuity at (x_0, t_0) which will be discussed in Sections 3-5.

In the construction of a fundamental solution we heavily refer to the convex and concave envelopes of the flux which are respectively given by

$$h(u; \bar{u}) := \sup_{\eta \in A(0,\bar{u})} \eta(u), \quad k(u; \bar{u}) := \inf_{\eta \in B(0,\bar{u})} \eta(u), \tag{11}$$

where

$$A(0, \bar{u}) := \{\eta : \eta''(u) \geq 0,\ \eta(u) \leq f(u) \ \text{ for } \ 0 < u < \bar{u}\}, \tag{12}$$

$$B(0, \bar{u}) := \{\eta : \eta''(u) \leq 0,\ \eta(u) \geq f(u) \ \text{ for } \ 0 < u < \bar{u}\}. \tag{13}$$

Note that we consider a positively signed fundamental solution and hence our interest is the flux on the domain $u \in [0, \infty)$ only which has been counted in the construction of envelopes.

One can easily check that, for any fixed $\bar{u} > 0$, $h(u; \bar{u})$ and $k(u; \bar{u})$ are convex and concave functions on the interval $(0, \bar{u})$, respectively. Since the flux function has only a finite number of inflection points, the domain $(0, \bar{u})$ can be divided into a finite number of subintervals so that envelopes are linear or identical to the flux on each subinterval. Employing these envelopes we summarize basic properties of a fundamental solution in the following lemma which is our main tool to see the dynamics of a fundamental solution.

Lemma 1 (structural lemma of a fundamental solution). *Let $u(x, t)$ be the positive source-type solution of the conservation law (1,2) with $M > 0$ and $\bar{u}(t) = \max_x u(x, t)$. For a given $t > 0$, let $0 = a_0 < a_1 < \cdots < a_{i_0} = \bar{u}(t)$ be the minimal partition of $(0, \bar{u}(t))$ such that the convex envelope $h(u; \bar{u}(t))$ is either linear or identical to $f(u)$ on each subinterval (a_i, a_{i+1}), $0 \leq i < i_0$. Similarly, let $0 = b_0 < b_1 < \cdots < b_{j_0} = \bar{u}(t)$ be the minimal partition related to the concave envelope $k(u; \bar{u}(t))$. Let $\zeta_0(t)$ is the maximum point in the sense that $\bar{u}(t) = \max(u(\zeta_0(t)+, t), u(\zeta_0(t)-, t))$ and $\mathrm{spt}(u(\cdot, t)) = [\zeta_-(t), \zeta_+(t)]$. Then,*

1. *The linear parts of the envelopes are tangent to the flux at intermediate partition points, i.e.,*

$$h'(a_i; \bar{u}(t)) = f'(a_i), \qquad i = 1, \cdots, i_0 - 1,$$
$$k'(b_j; \bar{u}(t)) = f'(b_j), \qquad j = 1, \cdots, j_0 - 1.$$

2. *The maximum $\bar{u}(t)$ is strictly decreasing as $t \to \infty$.*
3. *The solution $u(\cdot, t)$ increases on the interval $(\zeta_-(t), \zeta_0(t))$. Furthermore, if $h(u; \bar{u}(t))$ is linear on (a_i, a_{i+1}), there exists an increasing discontinuity that connects $u = a_i$ and $u = a_{i+1}$. If $h(u; \bar{u}(t)) = f(u)$ on (a_i, a_{i+1}), there exists a profile that continuously increases from $u = a_i$ to a_{i+1}.*

4. *The solution $u(\cdot,t)$ decreases on the interval $(\zeta_0(t),\zeta_+(t))$. Furthermore, if $k(u;\bar{u}(t))$ is linear on (b_j,b_{j+1}), there exists an decreasing discontinuity that connects $u=b_j$ and $u=b_{j+1}$. If $k(u;\bar{u}(t))=f(u)$ on (b_j,b_{j+1}), there exists a profile that continuously decreases from $u=b_{j+1}$ to b_j.*

Remark 1. There are many possible partitions $0=a_0<a_1<\cdots<a_{i_0}=\bar{u}(t)$ such that $h(u;\bar{u}(t))$ is either linear or identical to $f(u)$ on each subinterval (a_i,a_{i+1}), $0\le i<i_0$. However, the partition that consists of the smallest number of points is unique and we consider this minimal partition in the lemma. Then, clearly, if the envelope is linear in a subinterval, then it should be identical to the flux in the adjacent ones.

Lemma 1 provides useful information about the dynamics of the fundamental solution. First, if the maximum $\bar{u}(t)$ of the solution at a specific time $t>0$ is given, then the exact number of discontinuities and their left and right hand limits are easily computed. Furthermore, even though we do not know the exact place of the discontinuities from the lemma, we know how they are ordered. These discontinuities are connected by rarefaction waves. Notice that the rarefaction waves can be quite complicated if the flux is not convex and are not a function of x/t, which will be discussed in Section 5 (see Figure7). In Figure 1(a) an example of a convex and a

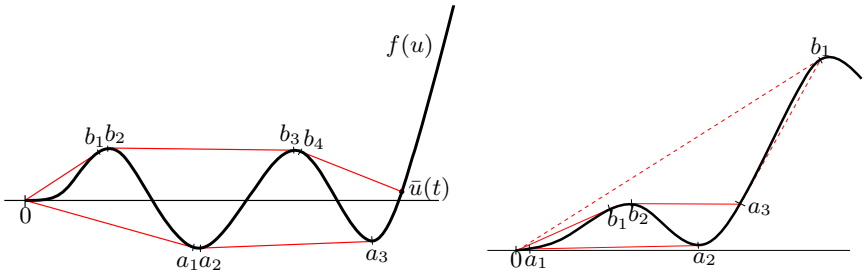

(a) convex and concave envelopes

(b) discontinuous change of envelopes

Fig. 1. Examples of envelopes. Minimal partitions consist of 0, $\bar{u}(t)$ and coordinates of the horizontal or u-axis of the tangent points. If both of the envelopes meet with linear parts as in (b), then the maximum jumps to the nearest interior partition point a_3 in the figure.

concave envelopes on the domain $[0,\bar{u}(t)]$ are given. Note that, since (5) is assumed, the graph of the flux function should be tangent to the x-axis at the origin. The minimal partition values a_i's for the convex envelope are marked at the corresponding tangent points which clearly show the relations in Lemma 1(1). Two linear parts of the convex envelope indicate that the fundamental solution have two increasing shocks. One of them jumps from 0 to a_1 and the other from a_2 to a_3. These shocks clearly satisfy the Oleinik entropy condition (3). Similarly the concave envelope and the corresponding minimal partition b_i's provide the decreasing shocks.

As the maximum $\bar{u}(t)$ of the fundamental solution decreases, the corresponding envelopes change continuously. However, if the point $(\bar{u}(t), f(\bar{u}(t)))$ reaches to a tangent point, then the envelopes change discontinuously and an example is given in Figure 1(b). The envelopes in dashed lines are the case when $\bar{u}(t) = b_1$. This implies that the maximum value $\bar{u}(t)$ is connected to the value a_3 by an increasing shock and also connected to 0 by a decreasing shock. In other words the solution has an isolated singularity which is not admissible. By the same reason the case $a_3 < \bar{u}(t) < b_1$ is not admissible. Therefore $\bar{u}(t)$ jumps from b_1 to a_3 and the envelopes evolve from the dashed ones to the solid ones in the figure. In particular the minimal partition for the concave envelope has new members and should be re-indexed.

3. Structure of discontinuities

In this section we classify shocks (or discontinuities) of fundamental solutions. The classification of discontinuity is given by the relation between the speed of the shock and the speeds of characteristic lines that emanate from the shock curve. Let $x = s(t)$ be a curve of discontinuity and $x = \xi_-(t)$ and $x = \xi_+(t)$ be characteristics lines that are connected to the discontinuity point $(s(t_0), t_0)$ from the left and the right hand side, respectively. If the discontinuity is admissible, then the speeds of these curves (or lines) should satisfy

$$\xi'_-(t) \geq s'(t_0) \geq \xi'_+(t). \tag{14}$$

The criterion of classification of discontinuities is if the inequality is strict or not. Therefore, there are four possible cases.

3.1. Genuine shock

If both of the inequalities in (14) are strict, then the discontinuity is called a genuine shock. If a faster characteristic line $x = \xi_-(t)$ collides to the slower shock curve $x = s(t)$ from the left hand side, it should come from the past (or as $t \uparrow t_0$). Similarly, the slower characteristic line $x = \xi_+(t)$ should collide to the shock curve from the right hand side as $t \uparrow t_0$. Therefore, for a genuine shock we have

$$\xi'_-(t) > s'(t_0) > \xi'_+(t) \quad \text{and} \quad t_0 - \varepsilon < t < t_0 \tag{15}$$

for some $\varepsilon > 0$. If one may take $t_0 - \varepsilon = 0$, then the characteristic lines are global, which is always the case with a convex flux.

We may easily see that a genuine shock of a fundamental solution connects the zero value and the maximum $\bar{u}(t) = \max_x u(x,t)$. If not, the discontinuity should connect a value of an intermediate partition point, say a_i. Since the shock speed $s'(t_0)$ is given by the relation in (9), Lemma 1(1) gives that

$$s'(t_0) = h'(a_j; \bar{u}(t)) = f'(a_j) = \xi'(t).$$

Therefore, at least one of the inequalities in (14) is not strict and hence the shock is not a genuine one. If a genuine shock connects the zero and the maximum, the corresponding envelope should be a straight line. Furthermore, since both of the envelopes can not be straight lines at the same time, a fundamental solution has at most one genuine shock. If a horizontal line is the convex or the concave envelope, then due to the normalization (5) one of the the inequalities are not strict. This is a transition stage of a genuine shock into a contact discontinuity which will be discussed in the following section for the dynamics of discontinuities.

Now suppose that a concave envelope is a non-horizontal line. Then the discontinuity connects the zero value and the maximum. We may easily see that if the line is not tangent to the graph of the flux, then it gives a genuine shock. Suppose that the line is tangent to the flux at the maximum as in Figure 1(b). Then the flux is locally concave at the maximum value $u = \bar{u}(t)$ and hence the convex envelope is also linear near the point. This implies that the maximum is an isolated singularity which is not admissible. Therefore, such an envelope does not exists. The same arguments may applied to the convex envelope and we may conclude the following.

Property 1. A positive fundamental solution has at most one genuine shock and it has one if and only if the convex or the concave envelope is a non-horizontal line. Furthermore the genuine shock always connects the maximum value and the zero state.

If the flux is convex, its concave envelope is simply a non-horizontal line and gives a decreasing genuine shock all the time. Furthermore, there are no other types of shocks for the convex flux. Figure 2(a) is an illustration of a genuine shock.

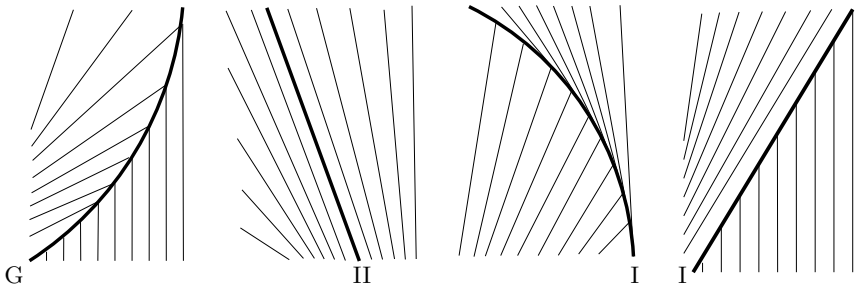

(a)genuine shock (b)type II contact (c)right contact (d)left contact

Fig. 2. Examples of shocks.

3.2. Contact shock

If a characteristic line that emanates from a discontinuity point is tangent to the discontinuity curve, then we call the discontinuity a contact

shock (or simply a contact). Let $a_i,\ i = 0, \cdots, i_0$, be the minimal partition in Lemma 1 related to the convex envelope h. One can easily see that if h is linear in an interior subinterval (a_i, a_{i+1}) (i.e., $a_i \neq 0$ and $a_{i+1} \neq \bar{u}(t)$), then Lemma 1(1) implies that both of the inequalities in (14) for the corresponding discontinuity are actually equalities. In this case the shock is placed between two rarefaction waves and hence it should be a straight line obviously. Since this discontinuity propagates with characteristic lines, it is not distinguished from the characteristics map. In this paper we call this contact shock type II (see Figure 2(b)). Note that we have mentioned the convex envelope only. In the following discussions we are going to stick to the convex envelope for consistency. However, there always exist their counterparts related to the concave envelope. In fact there is no reason to discriminate the concave envelope except the second hypothesis of (H1).

If one of the inequalities in (14) is actually an equality, then we call the contact shock of type I. A contact of type I is called a left contact if the left hand side inequality in (14) is actually an equality. Of course a right contact is the one of the other way. According to the previous discussions a contact of type I should connect the maximum or the zero value to an interior partition value. Since the maximum can not be connected by two shocks, the total number of contact shocks is as the following.

Property 2. A positive fundamental solution always has two or three contact shocks of type I counting a genuine shock as two. This means all the other shocks are of type II.

If a contact connects the zero value, then the slope of the corresponding linear part is not changing for a while (see Figure 1(a)), which is actually the speed of shock propagation. Hence the shock curve is a straight line. In Figure 2(c) an illustration of a left contact connecting the zero value is given.

The more interesting contact of type I is the one connecting the maximum. For example consider the linear part of the concave envelope in Figure 1(a) that connects the maximum $\bar{u}(t)$ and an interior partition value b_4. First note that the right hand side limit of the shock is b_4 by the entropy condition and that the speed of the characteristic line carrying this value is $f'(b_4)$ which is identical to the shock speed. Hence, the corresponding discontinuity is a right contact. One can easily see that the slope of the linear part decreases as $\bar{u}(t)$ decreases. Hence the shock curve should turn to the left hand side as t increases. Furthermore, the interior tangent value b_4 increases as $\bar{u}(t)$ decreases. This indicates that the range covered by rarefaction wave is increasing. In other words new information is produced and propagates to the future. Therefore, the characteristic line $x = \xi_+(t)$ connecting the shock from the right hand side goes to the future (or, in other words, the domain for the characteristic is $t_0 < t < t_0 + \varepsilon$ for some $\varepsilon > 0$). In Figure 2(d) this kind of right contact has been illustrated.

4. Dynamics of discontinuities

The convex and the concave envelopes have one end at the origin and the other end at the point $(\bar{u}(t), f(\bar{u}(t)))$, where $\bar{u}(t) = \max_x u(x,t)$ is the maximum value of the fundamental solution. Since the maximum $\bar{u}(t)$ decreases in time t, the envelopes and the corresponding minimal partitions are changing. In the followings we consider the dynamics of shock curves by tracking these changes. The change of envelopes is due to the decrease of the maximum value $\bar{u}(t)$ and hence only the part of the envelope between the maximum $\bar{u}(t)$ and the very next partition point can be changed as t increases.

Property 3. All the dynamics of shock discontinuities are produced along the shock curve that connects the maximum value of the positively signed fundamental solution.

4.1. Branching

A shock curve may split into two smaller shock curves or lines and we call this phenomenon a branching. Consider a shock curve that connects the maximum value $\bar{u}(t)$. Then it should be the genuine shock or of type I. If the corresponding linear part of the envelope touches a hump of the graph of the flux $f(u)$ on the way, it will split into two linear parts with a non-convex or a non-concave part in between. Since both of these two linear parts belong to the convex envelope or concave envelope, both shocks are increasing ones or decreasing ones. In other words an increasing shock splits into two increasing shocks and an decreasing one splits into two decreasing ones.

One can easily see that, at the moment that the branching process starts, the slope of the linear parts corresponding to the incoming and outgoing shocks are all the same. Therefore, the slopes of shock curves at the branching point in the xt-plane are identical and hence they form smooth curves.

It is clear that the split linear parts are tangent to the graph of the flux at one end. Since one of the linear part should have the maximum at its the other end, it gives a contact shock of type I. If the incoming shock is a contact of type I, then the other outgoing shock is of type II. Therefore, we may conclude that if the incoming shock is of type I, then, after a branching, it splits into one contact shock of type I and another one of type II (see Fig. 3(a), the horizontal axis for x and the vertical axis for t). Similarly, if the incoming shock is a genuine shock, then it splits into two contact shocks of type I (see Figure 3(b)). Note that type II cannot split.

4.2. Merging

Two shocks can be combined and then form a single shock. We call this phenomenon a merging. One can easily see this phenomenon from the

(a)Branching (I→I+II) (b)Branching (G→I+I)

Fig. 3. There are only two kinds of branchings.

change of envelopes. As the maximum value $\bar{u}(t)$ decreases, a linear part of convex envelope and a linear part of concave envelope may meet at a point, say $(\bar{u}(t_0), f(\bar{u}(t_0)))$. However, in this case it gives a removable jump (see Lemma 4.3 in [5]) and hence the maximum of the fundamental solution has a decreasing jump from $\bar{u}(t_0+)\big(:= \lim_{t\downarrow t_0} \max_x u(x,t)\big)$ to $\bar{u}(t_0-)\big(:= \lim_{t\uparrow t_0} \max_x u(x,t)\big)$. In this case $\bar{u}(t_0-)$ is the largest interior partition point (e.g., the point a_3 in Figure 1(b)). One can easily see that the slope of the linear parts of envelopes related these two incoming shocks and one outgoing shock are different and hence the shock curves are not smooth in general. The phenomenon related to this sudden change of envelopes will be discussed later for the aspect of a rarefaction wave.

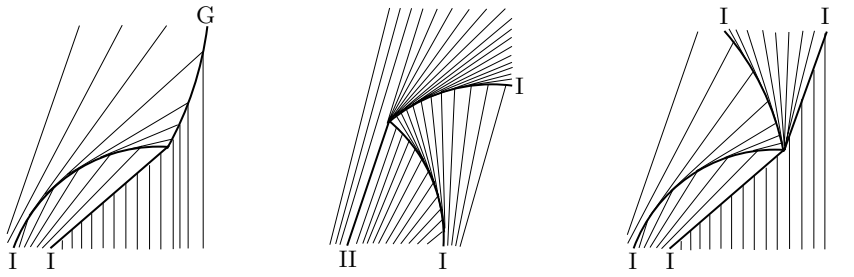

(a)Merging (I+I→G) (b)Merging (I+II→I) (c)Merging+Branching

Fig. 4. There are two kinds of merging. The last figure shows an example of a procedure when merging and branching occur simultaneously.

In Figure 4(a) two contacts of type I merge into a genuine shock. If contact shocks of types I and II are merged, then a contact of type I is produced (Figure 4(b)). These look like the opposite ways of the branching. However, the difference is that in the merging one increasing shock is merged with a decreasing one to produce another one. Note that, in branching, two shocks of the same monotonicity are produced. Another difference is that the shock curves are not smooth after the merging process.

4.3. Merging + Branching

The merging and the branching are basic phenomena in the dynamics of discontinuities. One may imagine the case that these two appear at the same time. Since the envelopes may change suddenly after a merging process, a branching may follow immediately after a merging. The example in Figure 1(b) is the case. Suppose that two incoming shocks meet at a point (x_0, t_0). Then the merging process produces one left contact and one right contact (see Figure 4(c)). Notice that the outgoing shocks should be of the same monotonicity. In this example they are given by the concave envelope and hence they are decreasing ones. It is also possible that there are more than two out going shocks. For example, if there are many wiggles in the inside hump of Figure 1(b), then there can be many outgoing shocks with same monotonicity with each other.

4.4. Transforming

A shock may change its type to a different one without branching or merging and we call this phenomenon a transforming. The only possible case is that a genuine shock is transformed to a contact shock of type I. As one can see in Figure 5(a), if a genuine shock changes its direction from the negative one to the positive one, then the genuine shock becomes a left contact. Similarly, if a genuine shock changes its direction of the positive one to the negative one, then it becomes a right contact. In Figure 4(a) two contacts of type I are merged into a genuine shock. If transforming happens simultaneously, then one may see the phenomenon that two contacts of type I are merged to produce a single contact of type I (see Figure 5(b)).

Remark 2. Notice that the phenomenon in Figure 5(b) is a special case of merging process. However, instead of placing it in the section for merging, we have it in this transforming section since it is based on the transforming process. Furthermore, the phenomena in this section can not be found under the extra hypothesis (H2). In fact, if the flux is positive, then the speed of the genuine shock is positive and hence transforming phenomenon does not appear. Therefore, under the extra hypothesis (H2), the dynamics of discontinuities is given by merging and branching only.

5. Structure of rarefaction waves

For the convex flux case there is no contact shock and hence all the characteristics of a fundamental solution carrying the information of a non-zero value are emanated from the origin. Then, if a fundamental solution u has a rarefaction profile at a point (x, t), the speed of the characteristic line that passes through the point is x/t and hence it should be satisfied that

(a)Transforming (b)Merging+Transforming

Fig. 5. Special phenomena without the hypothesis (H2).

$f'(u(x,t)) = x/t$. Furthermore, since f' is invertible if the flux is strictly convex, the rarefaction wave should be given by the following relation

$$u(x,t) = (f')^{-1}(x/t), \qquad a(t) \le x \le b(t), \tag{16}$$

where $[a(t), b(t)]$ is the support of the fundamental solution $u(\cdot, t)$. However, if the flux is not convex, then there may exist contact shocks and hence there are various possibilities for the starting point of the characteristic line. Furthermore, since f' is not invertible in the whole domain, one should clarify the correct profile that gives the rarefaction wave. In the followings we classify the rarefaction waves.

5.1. Centered rarefaction

There are two kinds of centered rarefaction waves. The first one is the one produced from the initial profile of the Dirac-measure and hence centered at the origin. Let $h(u;\infty)$ be the convex envelope of the flux and $0 = a_0 < a_1 < \cdots < a_{i_0} < \infty$ be the minimal partition. Then the rarefaction wave is given as

$$u(x,t) = g_\infty(x/t), \qquad a(t) \le x \le b(t),\ 0 < t < \varepsilon, \tag{17}$$

where the function $g_\infty(x)$ is piecewise continuous and satisfies $h'(g_\infty(x);\infty) = x$. Notice that the function $g_\infty(x)$ has discontinuity and hence $u(x,t)$ given by (17) has discontinuity which is actually contact shocks of type I or II. Therefore, the rarefaction wave in (17) should be understood as a sequence of rarefaction waves divided by contacts of type I or II. In Figure 7 an example of initial centered rarefaction wave can be found for $t > 0$ small. In the figure one may find that the waves are bounded by a genuine shock and a contact of type I. Then the inside profile is divided by a discontinuity of type II.

A centered rarefaction wave may also appear after a merging process. If a shock collides to another one, then the envelopes change suddenly and a centered rarefaction wave may appear. For example consider Figure 1(b) and suppose that two shock curves are merged at a point (x_0, t_0). Then

the concave envelope jumps from the dashed one to the solid ones and a nonlinear part in the interval (b_2, b_3) is added to the concave envelope, Figure 1(b), which generates a centered rarefaction wave given as

$$u(x,t) = g_1\big(\frac{x-x_0}{t-t_0}\big), \qquad \xi(t) \le x \le s(t),\ t_0 < t < t_0 + \varepsilon, \tag{18}$$

where g_1 is the inverse function of the derivative of the concave envelope of the flux on the domain (b_2, b_3) and the wave is bounded by a contact line of type I and a characteristic line, which are given by

$$\xi(t) = x_0 + f'(b_2)(t-t_0), \qquad s(t) = x_0 + \frac{f(b_1)}{b_1}(t-t_0),\ t_0 < t < t + \varepsilon.$$

The wave fan which is between two outgoing contacts of type I in Figure 4(c) and emanates from the branching point is a corresponding case.

One may also observe a centered rarefaction wave bounded by two characteristic lines. Consider the change of envelopes in Figure 6(d) after a merging. Then the interior partition point a_2 jumps from a_2^- to a_2^+ and a nonlinear part in the interval (a_2^-, a_2^+) is added to the convex envelope, which generates a centered rarefaction wave given as

$$u(x,t) = g_2\big(\frac{x-x_0}{t-t_0}\big), \qquad \xi_1(t) \le x \le \xi_2(t),\ t_0 < t < t + \varepsilon, \tag{19}$$

where g_2 is the inverse function of the derivative of the convex envelope of the flux on the domain (a_2^-, a_2^+) and the wave fan is bounded by two characteristic lines, which are given by

$$\xi_1(t) = x_0 + f'(a_2^-)(t-t_0), \qquad \xi_2(t) = x_0 + f'(a_2^+)(t-t_0),\ t_0 < t < t + \varepsilon.$$

Figure 4(b) is the corresponding figure. One may find a rarefaction wave fan centered at the merging point. The angle of this wave fan is same as the difference of slope of the incoming type II shock and outgoing left contact at the merging point.

In summary if a portion of the graph of the flux is added to the envelopes after a merging phenomenon, then a centered rarefaction wave appears.

Remark 3. The solution is continuous along the characteristic ξ_1, but not differentiable. This kind of regularity has been mentioned in Dafermos [2]. The rarefaction wave fan is bounded by a characteristic line at least one side. However, it is possible that there exist several contacts of type II inside of the fan.

5.2. Contact rarefaction

A centered rarefaction wave of a fundamental solution is produced at the moment of the initial time or of the merging. A contact rarefaction wave is produced continuously along the contact shock of type I if it is connected with the maximum value $\bar{u}(t)$. A typical example can be found

in Figure 6(a). The concave envelope in the figure shows that it is the moment that the genuine shock splits into two contact shocks of type I. The concave envelope at a later time is given in Figure 6(b), which shows that the rarefaction region (b_1, b_2) has been expanded. This indicates that new information has been produced and propagate to the future.

On the other hand the rarefaction region (a_3, a_4) for the convex envelope has been shrunken. In other words the information from the past disappears if it meets the shock. In summary the contact shock of type I connected to the maximum erases the information of the past from one side and produces new information from the other side.

6. Example for the dynamics of a fundamental solution

In this section we consider an example of a complete characteristic map that shows all the dynamics of shocks and rarefaction waves discussed before. We take a flux in Figure 6 which is complicate enough for this purpose. Since the change of an envelope is linked to each stage of a solution, all the dynamics of a solution can be interpreted in terms of envelopes. First eight figures in Figure 6 are the envelopes of the flux corresponding to the possible eight stages of the fundamental solution. As an example to show this connection we put an illustration of a positive N-wave in Figure 6(i), which belongs to the second stage, Figure 6(b). More examples of N-waves can be found in [5], Figures 6, 7 and 8, which are actually obtained by computing the equation numerically. A complete characteristic map corresponding to this flux is given in Figure 7 with stage numbers on the left. In the rest of this section we discuss on the relation between the flux and its characteristic map.

Due to the second hypothesis in (H1), one can find a moment t_0 such that for all positive $t < t_0$ the concave envelope consists of a single non-horizontal line. In the case there exists a decreasing genuine shock as denoted in Figure 6(a). In addition, there are two increasing shocks from the very beginning, one of type I (right contact) and the other of type II. These shocks are connected by two wave fans centered at the origin.

As t increases, the right contact and the type II shock moves with a constant speeds which are the slope of the corresponding linear parts of the envelopes in 6(a). However, the slope of the concave line corresponding to the genuine shock decreases and hence the shock curve is not linear as one can find in Figure 7. On the way, we watch two branchings (G→L+R, R→II+R) in the evolution of the concave envelope while the convex envelope has no such changes until the fourth stage, see Figures 6(b) and (c). Note that at every branching point all the curves and the line have the same slope as shown in Figure 7.

After then, we may observe three merging phenomena (II+R→L, L+II→R, R+R→G) as illustrated in Figures 6(d)–(f). Note that at every merging point none of two curves and the line have the same slope. In addition,

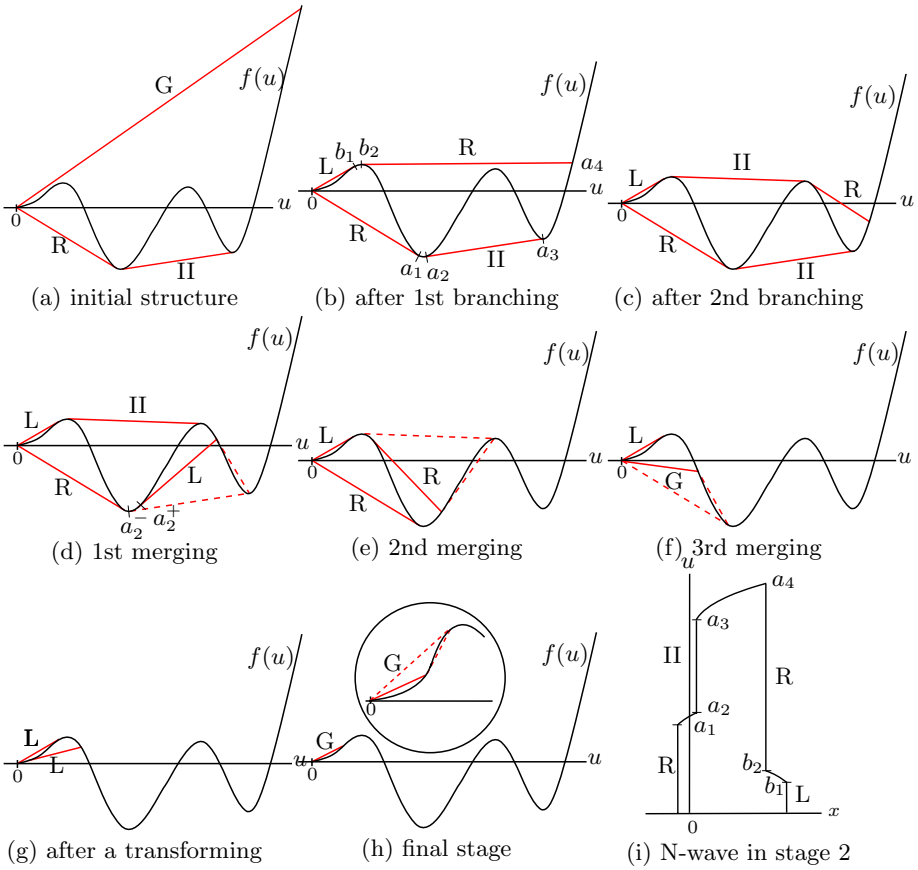

(a) initial structure (b) after 1st branching (c) after 2nd branching

(d) 1st merging (e) 2nd merging (f) 3rd merging

(g) after a transforming (h) final stage (i) N-wave in stage 2

Fig. 6. The envelopes of all eight stages. As the maximum of the fundamental solution decreases the corresponding envelopes change. G: genuine shock, R: right contact of type I, L: left contact of type I, II: contact of type II. a_j, b_j in (b), (d) for horizontal coordinates but vertical in (i).

centered wave fans appear after the first two mergings. However, if a genuine shock is produced, any kind of rarefaction waves is not produced. This genuine shock moves to the left slower and slower (very steep in Figure 7 because x is on the horizontal line) until it reaches the speed of zero and then the genuine shock turns into a left contact which moves to the right, see Figures 6(g) and 7. (Note that it is possible that, after the third merging, Figure 6(f), a left contact may appear instead of the genuine shock and directly go to the stage 7 of Figure 6(g), which is the case discussed in Figure 5(b).) Finally, this left contact meets with the other left contact after a long time and generates a genuine shock as in Figure 6(h). The picture in the circle shows the final merging process. From this moment this genuine shock is a unique discontinuity and persists forever.

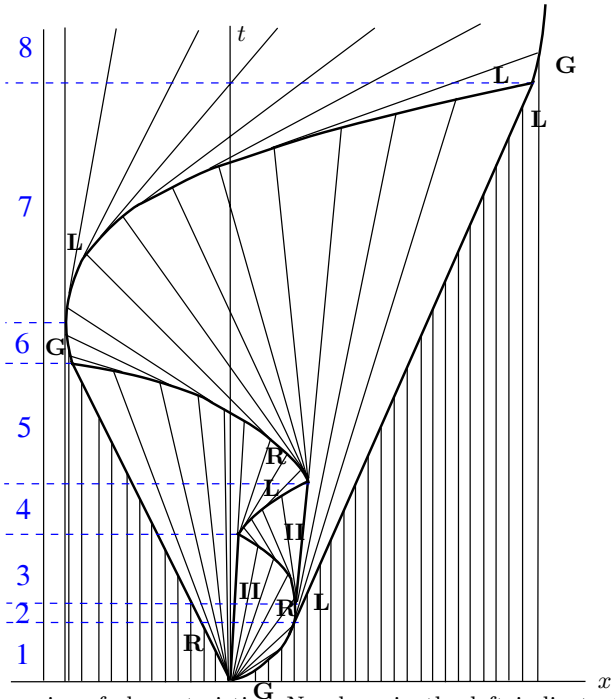

Fig. 7. Dynamics of characteristics. Numbers in the left indicate the stage of each strip.

Note that Figure 6 is for an illustration purpose and made under certain exaggerations to keep the whole dynamics in a single figure. It seems interesting to compare this illustration with a one obtained from an actual solution. In fact, we have computed a fundamental solution numerically and then displayed its dynamics in Figures 8 and 9. In the figure we have displayed up to the beginning of Stage 7.

In Figure 8 the vector fields $(f'(u), 1)$ is given after a normalization, where u is a numerically computed fundamental solution. Then, clearly, the integral curves are the characteristics of the solution. Shock curves are formed at the place that the vectors collide to each other. One may observe the shock curves and easily distinguish if it is a left contact or a right contact. This shock curves matches with Figure 7 pretty well except the ones near the initial time. For $t > 0$ small the evolution of the solution is fast and one may observe numerically if the corresponding part is magnified which is omitted here.

In Figure 9 simply the wave speed $f'(u)$ is plotted for the same numerical solution. In this figure the appearance of the centered rarefaction waves and propagation of discontinuities discussed before are more clearly observed. To produce these figures we used MATLAB fucntions such as 'quiver' and 'contourf' for a numerical solution obtained using WENO method. Theses

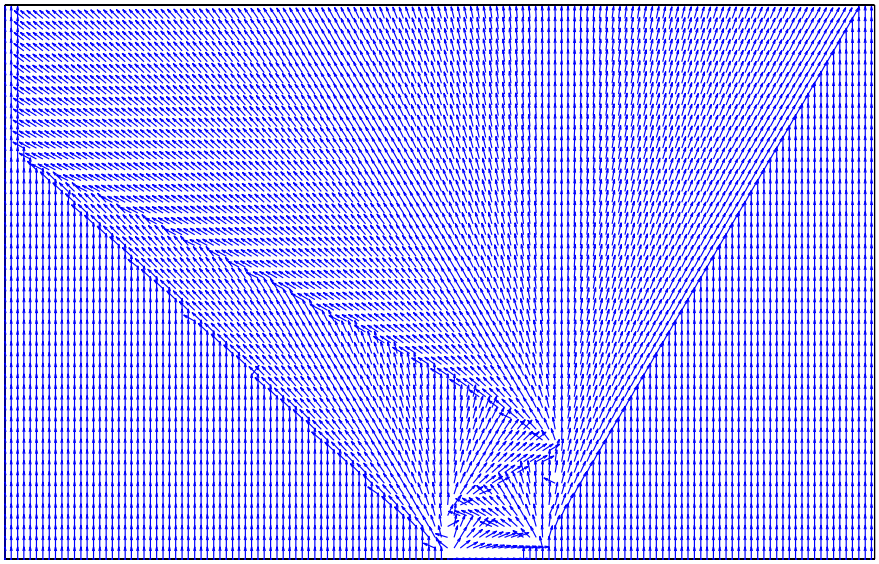

Fig. 8. The vector field for characteristic curves is plotted for a numerical solution. An integral curve of it is a characteristic curve. Collision of this vector field indicates shock curves.

figure indicates that the theoretical explanation and the numerical simulation matches well.

7. Flux under positivity

In this section we consider effects of the positivity of the flux and consider a flux that satisfies

$$f(u) \geq 0 \quad \text{for} \quad u \in \boldsymbol{R}. \tag{H2}$$

7.1. Positive fundamental solutions

Under this positivity hypothesis there are several limitations in the evolution of the fundamental solution and hence certain phenomenon does not appear and the solution becomes simpler. In this section we discuss these differences.

First one can easily see that the convex envelope $h(u;\bar{u}(t))$ is never a non-horizontal line in the subinterval $(0, a_1)$. Since a contact of type I should be connected to the zero value or the maximum, there always exist two contacts of type I counting a genuine shock as two. The positivity of the flux gives that the convex envelope satisfies $h'(u) \geq 0$ for all $u \geq 0$. Therefore, the increasing shocks move to the right and hence the support of the solution is on the positive side, i.e., $\mathrm{spt}(u(\cdot,t)) \subset [0,\infty)$.

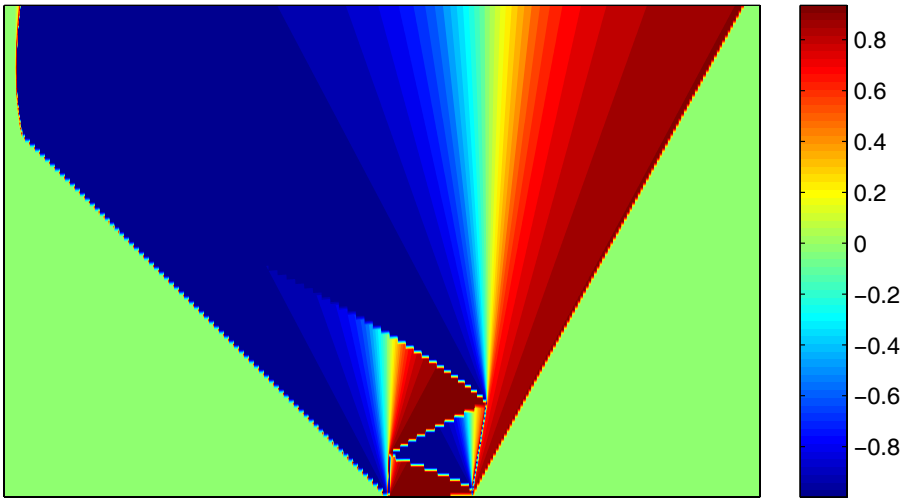

Fig. 9. The display of the wave speed of the same numerical solution shows generation of centered rarefaction waves and interaction of contacts more clearly.

If the fundamental solution has a genuine shock, then the concave envelope should be the line connecting the origin and the maximum point $(\bar{u}, f(\bar{u}))$ which should have a strictly positive slope due to (H2). In other words a genuine shock always moves to the right. Hence the transforming phenomenon in Section 4.4 does not appear and all the dynamics of a fundamental solution are generated by branching and merging.

In summary, under (H2), there are a unique genuine shock and a finite number of contact discontinuities of type II at the beginning stage. Note that contact shock of type I does not appear at this early stage. Then one might observe two types of branching given in Section 4.1 and two types of merging given in Section 4.2 in the intermediate stages. In the final stage, two contacts of types I merge and produce a genuine shock.

7.2. N-waves

It is natural to ask if the signed fundamental solution considered before is the unique solution of the Cauchy problem (1,2). The uniqueness of the solution obtained by Krushkov [6] is a solution with a bounded initial value and it does not imply the uniqueness of a fundamental solution. In fact the N-waves $N_{p,q}(x,t)$ given in (4) are solutions for all $p, q \geq 0$ such that $q - p = M$ if the flux satisfies the extra hypothesis (H2). Since the negative part and the positive part of the solution evolves independently, there is no additional structure to be mentioned about these sign-changing solutions.

Acknowledgements. Authors would like to thank Youngsoo Ha and Seunghoon Jung for useful discussions and their help in making several feagures in this paper.

References

1. D.P. Ballou, *Solutions to nonlinear hyperbolic Cauchy problems without convexity conditions.* Trans. Amer. Math. Soc. **152** (1970), 441–460.
2. C.M. Dafermos, *Regularity and large time behaviour of solutions of a conservation law without convexity.* Proc. Roy. Soc. Edinburgh Sect. A **99** (1985), 201–239.
3. M. Kim and Y.-J. Kim, *Invariance property of a conservation law without convexity.*
4. Y.-J. Kim, *Potential comparison and asymptotics in scalar conservation laws without convexity.* J. Differential Equations **244** (2008), 40–51.
5. Y.-J. Kim and Y. Ha, *Fundamental solutions of a conservation law without convexity.* preprint at http://amath.kaist.ac.kr/∼ykim/preprints/14.pdf
6. S. N. Krushkov, *First-order quasilinear equations with several space variables.* Mat. Sb., **123** (1970), 228–255.
7. T.-P. Liu, *Admissible Solutions of Hyperbolic Conservation Laws.*Mem. Amer. Math. Soc. **240**, AMS, Providence, RI, 1981.
8. T.-P. Liu, M. Pierre, *Source-solutions and asymptotic behavior in conservation laws.* J. Differential Equations **51** (1984), 419–441.
9. T. Tang, Z.-H. Teng and Z. Xin, *Fractional rate of convergence for viscous approximation to nonconvex conservation laws.* SIAM J. Math. Anal. **35** (2003), 98–122.

Yong-Jung Kim
Department of Mathematical Sciences, KAIST
335 Gwahangno,Yuseong-gu, Daejeon 305-701, Republic of Korea
email:yongkim@kaist.edu

and

Young-Ran Lee
Department ofMathematical Sciences, KAIST
335 Gwahangno, Yuseong-gu, Daejeon305-701,Republic of Korea
email:youngranlee@kaist.ac.kr